Tunable coherent Ising machines with fifth-order nonlinearity

Ruqi Shi
Photonics Research Group
Ghent university
Ghent, Belgium
Email: Ruqi.shi@ugent.be

Thomas Van Vaerenbergh
Hewlett Packard Labs
Diegem, Belgium
Email: thomas.van-vaerenbergh@hpe.com

Fabian Böhm
Hewlett Packard Labs
Boeblingen, Germany
Email: fabian.bohm@hpe.com

Peter Bienstman
Photonics Research Group
Ghent university
Ghent, Belgium
Email: Peter.bienstman@ugent.be

***Abstract*—Ising machines offer fast and energy-efficient computational capabilities as next-generation hardware accelerators for combinatorial optimization problems. We have developed numerical coherent Ising machine (CIM) models that utilize a fifth-order polynomial transfer function. This model has the potential to be implemented in photonic platforms and allows for both supercritical and subcritical pitchfork bifurcation operational regimes. This provides an additional tunable hyperparameter to control the Ising spin dynamics compared with the common third-order polynomial CIM model. Moreover, the hysteresis observed in the subcritical pitchfork operational regime can be utilized for noise suppression. In our benchmark studies, we simulated various sizes of MaxCut problems using the fifth-order polynomial CIM model without any error correction algorithms. The results showed a significant improvement from the subcritical pitchfork CIM model compared with the normal form third-order polynomial CIM model, achieving 23 out of 30 Maxcut instances with an average of 60% increased success rate. The advantages are more pronounced in large instances with N=80, 100. Our results indicate that involving more tunable hyperparameters and enabling hysteresis with large noise in the optimization process enhances the computational power of the Ising machine.**

I. Introduction

The Ising model, known for its versatility in both theoretical and practical contexts, stands as a fundamental pillar in statistical mechanics. It provides invaluable insights into the behavior of interacting particles in various physical systems. It is depicted as an undirected graph, comprising a collection of binary Ising spin nodes ($x_i = \pm 1$) interconnected by Ising coupling interactions denoted as J_{ij}. The Ising Hamiltonian is mathematically expressed as $H = -\frac{1}{2}\sum_{i \neq j} J_{ij} x_i x_j$. When solving an Ising problem, the primary objective is to determine spin configurations that minimize the Ising Hamiltonian, given a specific coupling interaction matrix. A generic Ising problem belongs to the category of NP-hard combinatorial optimization problems, indicating that it cannot be solved in polynomial time with respect to the problem size N (i.e. the number of nodes in the Ising model) and thus requires exponential computation time to solve on a classical computer. Due to the NP-hard nature, Ising problems have the potential to encode other NP-hard combinatorial optimization problems such as Maxcut problems and traveling salesman problems.

The operational principle of an Ising machine is to solve Ising problems by implementing an Ising model and minimizing its Ising Hamiltonian over time. Figure 1 provides an example of the workflow of using an Ising machine as a Maxcut solver.

In this work, we present the simulation of a novel designed Integrated Ising machine model that can be fabricated on photonic integrated circuits [1]. The main novelty lies in the consideration of a fifth-order nonlinearity to have more hyperparameters and a large noise regime to facilitate exploration.

II. Integrated CIM model

As an important type of Ising machine, considerable attention has been paid to coherent Ising machines (CIMs) [2]–[4], which consist of a network of optical Ising nodes with bistable states of coherent light pulses (e.g., 0 and π phases, or the in-phase amplitude of the coherent light pulses). However, most of the CIMs are based on optical parametric oscillators (OPOs), requiring large experimental setups. As a compact Ising machine implementation, integrated CIMs have been proposed in recent work [1]. A schematic of an integrated CIM on a photonic integrated circuit can be seen in Figure 2.

The time differential equation for each spin amplitude in the integrated CIM system can be approximated as a fifth-order polynomial transfer function [1]:

$$\dot{x_i} \approx \underbrace{(r-1)x_i - \eta x_i^3 + \zeta x_i^5}_{\text{fifth-order nonlinear dynamic function}} + \underbrace{\beta \sum_{j}^{N} J_{ij} x_j}_{\text{linear coupling function}} + \underbrace{\gamma c\,(0,1)}_{\text{random noise}}, \; i = 1, 2, \cdots, N. \tag{1}$$

Here, x represents the light amplitude or analog spin amplitude with the sign indicating the binary spin direction. r is the linear gain, η and ζ are the third-order and fifth-order coefficients respectively. .γ is the noise level. r, η, ζ, and γ are tunable hyperparameters in our fifth-order CIM model which can be further optimized for specific problems. The fifth-order nonlinearity comes from the nonlinearity of the microrings on the photonic circuit [1] and enables supercritical and subcritical operation regimes with hysteresis in the bifurcation diagram, which can be seen in Figure 3 for supercritical regime and Figure 4 for subcritical regime.

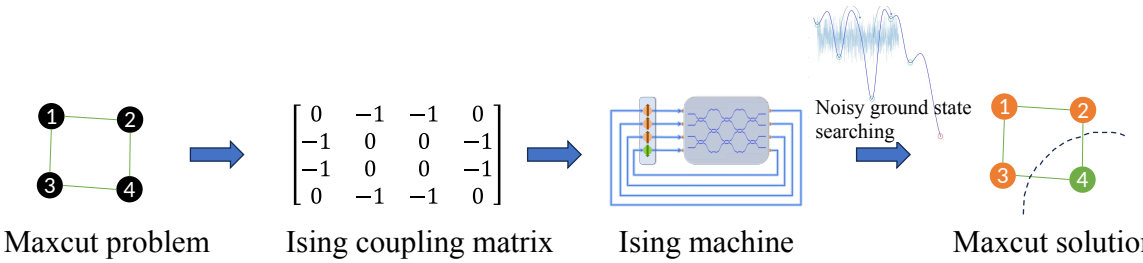

Fig. 1. Workflow of an Ising machine as a Maxcut solver: starting from a Maxcut problem defined by a certain undirected graph, the problem is then encoded into an Ising coupling matrix, which will be fed into an Ising machine with optimized hardware to this specific problem. By the noisy ground state search process, if the Maxcut problem is solvable, after an evolution time, the Maxcut solution will be finally returned as the ground-state Ising spin configuration.

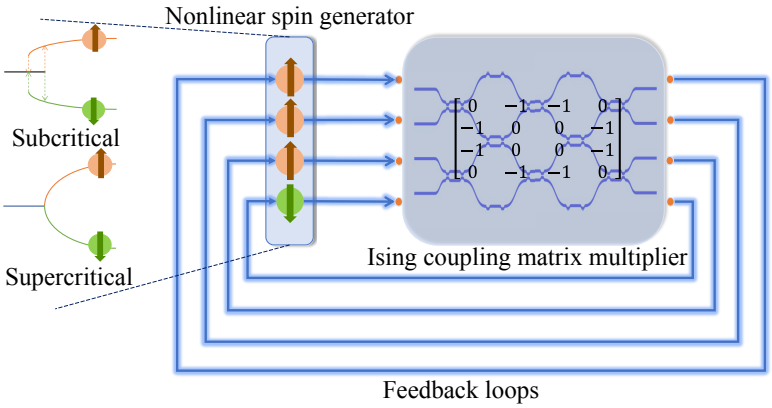

Fig. 2. Schematic of an integrated CIM on a photonics integrated circuit: three main building blocks are involved, including a nonlinear spin generator, an Ising coupling matrix multiplier, and feedback loops. The Ising machine can either be operated in subcritical pitchfork regime or supercritical pitchfork regime. The nonlinear spins and matrix multiplier can be realized by microring resonators and MZI mesh on a photonic integrated circuit.

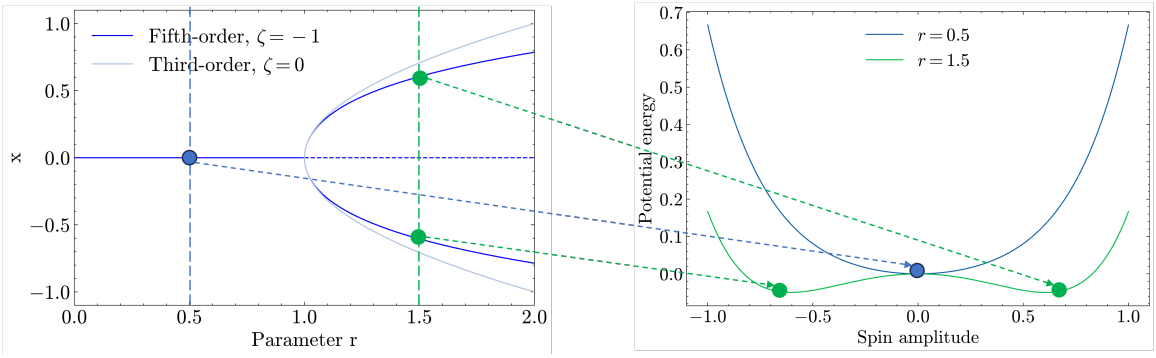

Fig. 3. Left: operational bifurcation diagram for spin dynamic function $\dot{x} = (r-1)x - x^3 + \zeta x^5$ in the supercritical (i.e. $\eta > 0$) pitchfork regime. Right: potential energy curves correspond to points below or above the supercritical pitchfork bifurcation point.

Hysteresis is a phenomenon in which a system experiences a time lag in response to external changes in input or operating conditions. This lag can be likened to a "memory effect" of the system, which can potentially enhance the system's robustness against external random noise. Therefore, we will engineer the hysteresis by tuning the Ising machine hyperparameters in a large noise regime, to exploit its potential computational power.

III. Results

To evaluate the computational performance and scalability of the fifth-order polynomial CIM model, we solve benchmark MaxCut problems of size $N = 60, 80, 100$ with 50% edge density from the BiqMac benchmark tasks [5]. We compare the time-domain simulation and success rate results with the normal form third-order polynomial model in [6].

A. Time-domain simulation

To further validate the hypothesis that hysteresis in the subcritical regime can reduce fluctuations and enhance the noise immunity of the Ising machine, we conducted a time-domain simulation. We focused on the spin amplitude and energy evolution of the BiqMac instance $g\_05\_100.6$ as a representative example.

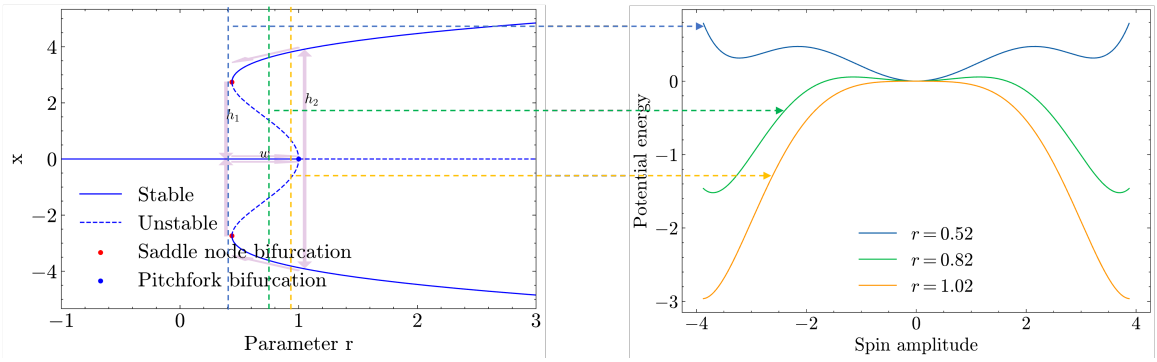

Fig. 4. Left: operational bifurcation diagram for spin dynamic function $\dot{x} = (r-1)x + 0.15x^3 - 0.01x^5$ in subcritical pitchfork regime ($\eta > 0$ and $\zeta < 0$), hysteretic loops are depicted by purple arrows. Right: three potential energy curves correspond to three r values below or above the subcritical pitchfork bifurcation point.

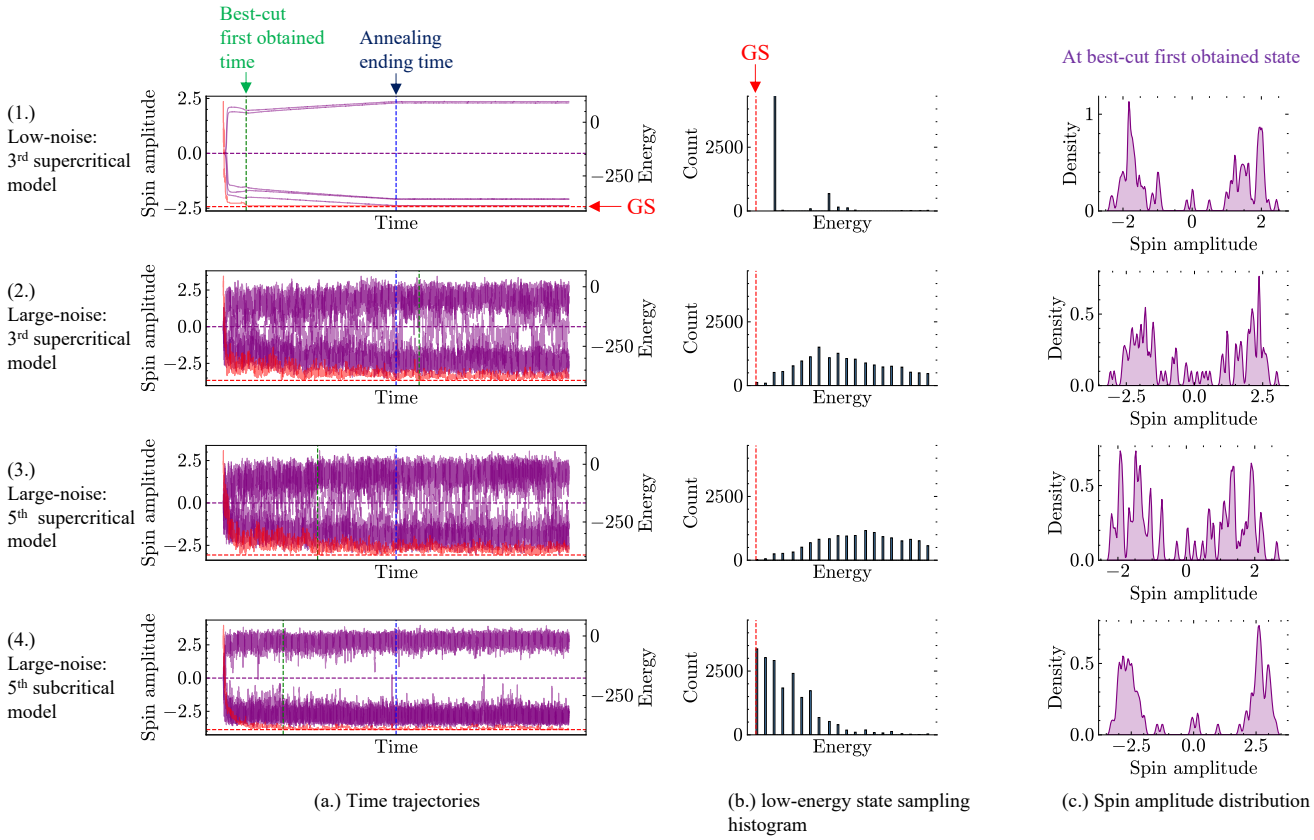

Fig. 5. Time trajectories and related statistical analysis of CIM models under low and large noise profiles for BiqMac instance $g\_05\_100.6$ with $N = 100$ Ising nodes. Row (1.) shows the low noise level simulation for the third-order supercritical model with $\gamma = 0.01$. Row (2-4) show the large noise level simulation of third-order supercritical model, fifth-order supercritical model, and fifth-order subcritical model with $\gamma = 2$, respectively. Column (a.) presents the evolution of energy which is represented by the red curve and spin amplitude which is represented by the purple curves (only 5 randomly selected nodes out of 100 nodes are displayed for clarity). Column (b.) displays the histogram of the low-energy state samplings (from the ground state energy to 90% ground state energy) during simulation. Column (c.) shows the spin amplitude density distribution of all 100 Ising nodes at the best-cut first obtained state, demonstrating the analog heterogeneity of each model when reaching the optimal solution during a run. The model parameters for the simulation have been optimized by the hyperparameter optimization process.

Figure 5 shows the time trajectories under large noise profiles with corresponding statistics of energy and spin-amplitude distribution for the third-order model in row (2.), supercritical fifth-order model in row (3.), and subcritical fifth-order model which is operated under the hysteresis regime in row (4.). A low noise simulation of the third-order model is also presented in row (1.) as the control subject for studying the performance enhancement resulting from the fifth-order nonlinearity and large noise. The time trajectories in column (a.) show that the third-order model under a low noise level

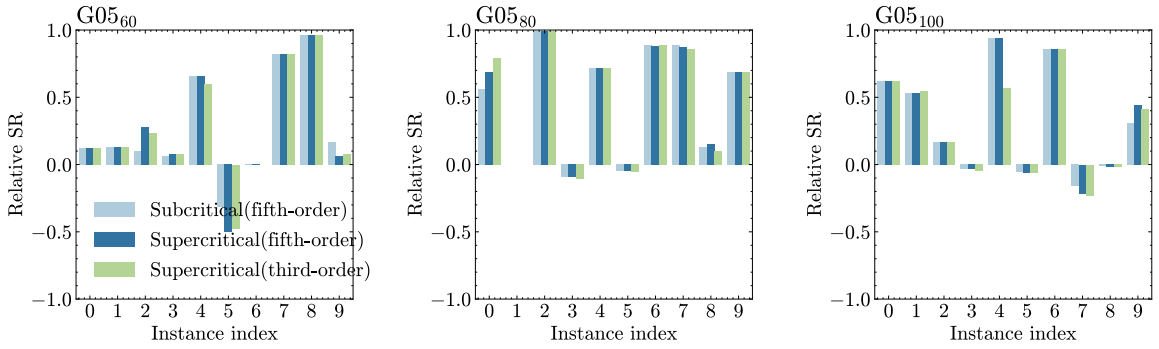

Fig. 6. Relative success rate (SR) for Biqmac Maxcut instances with $N = 60, 80, 100$ nodes and 50% edge density, compared with simulation results of the normal third-order CIM in [6]. The SR refers to the probability of finding the ground state during one simulation trial, which was obtained by 200 trials per instance. A positive relative SR means a higher SR compared with the normal third-order CIM result.

exhibits clean time traces and traps in a local minimal energy state quickly. The large noise simulation shows much noisier behavior in the spin dynamics. Among the three models, the subcritical model in the bottom row shows the fastest attainment of the ground state and generates fewer spin flips after reaching the ground state compared to the other two models. The supercritical model with the same fifth-order coefficient as the subcritical model (middle row) behaves the worst in terms of solving speed and immunity against random spin flipping. Turning our attention now to the histogram of the low-energy state samplings in column (b.), we see that the third-order model under a low noise level spends most of the time in a low-energy state near the ground state but unable to reach the ground state. For the large noise level simulation, the subcritical model shows a large concentration of low-energy states during simulation, indicating a tendency to remain in these states. On the other hand, the other two models have a higher probability of sampling higher-energy states. This trend further supports the superiority of the subcritical model in terms of low-energy state sampling efficiency. Finally, column (c.) illustrates the spin amplitude distribution for the state when the best-cut is first obtained. The results suggest that the subcritical model under a large noise level has a smaller standard deviation of spin amplitudes for both negative and positive spin directions, with fewer amplitudes around the flipping threshold compared to the other two models, even better than the low noise simulation of a third-order model.

B. Success rate

After the optimization of the Ising machine hyperparameters, the relative success rate (SR) results shown in Figure 6 illustrate that the fifth-order CIM model outperforms the normal third-order OPO CIM model in 23 out of 30 Maxcut instances with an average of 60% increased SR. The advantages are more pronounced in large instances with $N = 80, 100$. This indicates that involving more tunable hyperparameters and enabling hysteresis with large noise in the optimization process enhances the computational power of the Ising machine.

IV. Conclusion

In this study, we investigate the advantage of implementing fifth-order polynomial CIM models. Our simulation shows that the fifth-order subcritical CIM model with hysteresis is more resistant to high levels of noise compared to the supercritical CIM models. By tuning and optimizing the model parameters, we have significantly improved the computational performance on benchmark problems in the BiqMac library. The fifth-order CIM model has achieved a 60% increase in success rate on 23 out of 30 Maxcut instances, compared to the standard third-order polynomial CIM model, especially in larger instances with N=80, 100. These findings provide strong evidence for the computational advantages of the proposed fifth-order polynomial CIM model.

Acknowledgment

The authors would like to gratefully thank the support from Belgian EOS project Pinch.

References

[1] N. Tezak, T. Van Vaerenbergh, J. S. Pelc, G. J. Mendoza, D. Kielpinski, H. Mabuchi, and R. G. Beausoleil, "Integrated coherent ising machines based on self-phase modulation in microring resonators," *IEEE Journal of Selected Topics in Quantum Electronics*, vol. 26, no. 1, pp. 1–15, 2019.

[2] Z. Wang, A. Marandi, K. Wen, R. L. Byer, and Y. Yamamoto, "Coherent ising machine based on degenerate optical parametric oscillators," *Physical Review A*, vol. 88, no. 6, p. 063853, 2013.

[3] T. Inagaki, K. Inaba, R. Hamerly, K. Inoue, Y. Yamamoto, and H. Takesue, "Large-scale ising spin network based on degenerate optical parametric oscillators," *Nature Photonics*, vol. 10, no. 6, pp. 415–419, 2016.

[4] Y. Haribara, Y. Yamamoto, K.-i. Kawarabayashi, and S. Utsunomiya, "A coherent ising machine with quantum measurement and feedback control," *arXiv preprint arXiv:1501.07030*, 2015.

[5] A. Wiegele, "Biq mac library—a collection of max-cut and quadratic 0-1 programming instances of medium size," *Preprint*, vol. 51, 2007.

[6] F. Böhm, T. V. Vaerenbergh, G. Verschaffelt, and G. Van der Sande, "Order-of-magnitude differences in computational performance of analog ising machines induced by the choice of nonlinearity," *Communications Physics*, vol. 4, no. 1, p. 149, 2021.